Indian Journal of Chemical Technology
Vol. 32, March 2025, pp. 272-279
DOI: 10.56042/ijct.v32i2.7208

A comparative study on removal of As(III) from industrial wastewater using newly synthesized polysaccharide-based chelating resins

Abhishek Solanki, Anju Chowdhary, Sawai Singh Rathore & Vikal Gupta*

Department of Chemistry, Jai Narain Vyas University, Jodhpur-342001, Rajasthan, India

*E-mail: vikal_chem@yahoo.co.in

Received 8 December 2023; accepted 3 February 2025

Water contamination by a wide range of hazardous substances including heavy metals, metalloids, and dyes is a major environmental concern due to their potential human toxicity. Therefore, technologies for the removal of harmful contaminants in wastewater have been developed substantially. Among all the methods that have been proposed, ion exchange and adsorption processes are the most efficient techniques for removal of contaminants from industrial wastewater and very important tools for environmental protection also. In this study, we focus on removing As(III) by applying an ion exchange mechanism using TKP (Tamarind kernel powder) and CCSP (*Citrullus Colocynthis* seed powder) based chelating resin. FTIR spectra & SEM analysis confirm the functional groups and structure of newly synthesized resins subsequently. With the use of the Langmuir and Freundlich isotherm models, the interaction of metalloid ion with chelating resin has been evaluated. Effects of various parameters like contact time, chelating resin dosage, metalloid ion concentration, and pH on removal efficiency are also discussed. The maximum removal efficiencies of TTABA (Tamarind Triazine Amino Butanedioic Acid) resin and CTABA (Citrullus Triazine Amino Butanedioic Acid) resin have been observed as 82.3% and 75.6%, respectively, for As(III).

Keywords: Adsorbents, Adsorption, Biopolymers, Chelating resin, Ion exchange method, Pollutants, Polysaccharides

Introduction

The most significant environmental issue is contamination of water that is being faced by living beings on Earth. Rapid population growth, urbanization, and industrialization release enormous volumes of wastewater into water bodies and the uncontrolled disposal of various chemicals and substances contaminate the water, and substantially change the water quality of natural water bodies[1]. The contamination often creates long-term adverse effects on the aquatic life and human health and thus becoming less suitable for drinking, domestic, agricultural, industrial, recreational, wildlife, and other uses. Industrial wastewater possesses biodegradable and non-biodegradable organic matter, oils and fats, heavy metals, saltwater or brines. Water bodies contaminated by industrial effluents with high levels of heavy metals can cause heavy metal poisoning, gastrointestinal illnesses, skin irritation, liver, or kidney damage, and death[2,3].

Heavy metal ions pose an environmental threat due to their cumulative, toxic, and non-biodegradable characteristics[4,5]. Arsenic is one of the toxic elements that can be found in industrial waste[6]. Arsenic is frequently employed in a variety of industrial operations, such as the production of pesticides, wood preservation, and metalloid smelting. Arsenic-containing industrial waste is inappropriately dumped into bodies of water which can contaminate the water, destroy aquatic life, and endanger human health[7]. Arsenic can enter the environment in several ways, such as accidental spills, waste disposal site leaching, and emissions into the atmosphere from industrial facilities. When arsenic enters the environment, it can accumulate in the soil and water and be ingested by plants, animals, and even fishes that humans eat.

Exposure to arsenic can result in skin lesions, cardiovascular illness, and several cancers, including bladder, skin, and lung cancer. The detrimental effects of arsenic exposure on health are particularly dangerous for children and pregnant women[8]. The extraction of As(III) from water is crucial due to its serious health and environmental hazards. As(III) is extremely toxic and recognized as a carcinogen, with prolonged exposure linked to a range of cancers, heart diseases, and neurological impairments. Its occurrence in drinking water, especially in areas with contaminated groundwater such as parts of South

Asia, represents a significant public health risk. As(III) is more soluble and mobile in water compared to As(V), which complicates its removal and heightens the risk of widespread contamination. It is vital to effectively eliminate As(III) to comply with regulatory standards, safeguard human health, and provide safe drinking water[9]. Since arsenic poses a major risk to both the environment and human health, there have been several studies on its removal from wastewater. In recent studies, polysaccharides-based adsorptive resins have been widely designed to remove metalloids from industrial wastewater. Chemical polymerization is the chemical process of establishing smaller monomers to make bigger macromolecules that form a polymer, which is used to introduce functional groups into natural polysaccharides for improving their adsorption capacity. The presence of hydroxyl, carboxyl, carbonyl, ether or amino like chemical reactive functional groups in polymer chain show high reactivity as well as selectivity towards heavy metal ions[8].

Chemical precipitation, advanced oxidation processes, membrane filtration, ion exchange, adsorption and coagulation-flocculation[10–12] are the conventional methods used to remove heavy metal ions from industrial waste water. These techniques are found to be effective for waste water treatment but most of them are neither economically viable due to high operational cost, high chemical requirements, maintaining ideal pH levels etc. nor environmentally friendly due to extensive sludge production and disposal of the toxic sludge. While flexibility in design and operation, sorption processes such as adsorption and ion exchange are considered as the most effective, inexpensive, environmentally safe processes and boasts high treatment capacity and high metal removal rates, making it highly efficient in reducing heavy metals to acceptable levels[13]. The treated water via these processes is colorless, odorless, and suitable for reuse.

In compared to other procedures, chelation ion exchange has various advantages including high removal efficiency, low expenses, no production of chemical sludge, and ease of accessibility, which renders it one of the best physicochemical methods for disposing of heavy metal ions[14]. In addition, during the removal process of the toxic metal ions, harmless ions are filtered and released into the environment. Moreover, chelation ion exchange indicates the formation of coordination bonds between heavy metal ions and chelating polymers[15]. These materials pose a risk of secondary pollution to the environment because of their non-biodegradable nature. Therefore, researchers from all over the world are trying to synthesize environmental-friendly, low cost and highly efficient bio-polymers based on natural products for treatment of industrial wastewater. The effectiveness of various techniques for removing arsenic from wastewater has been the subject of a few studies, and the optimal conditions for each technique, including pH, coagulant dosage, and contact time, have all been investigated. The key objective of this study is to compare the chelation efficiencies of TKP and CCSP-based biopolymers for the removal of As(III) metalloid ion using various parameters such as metalloid ion concentration, adsorbent dose, pH, particle size, and contact time. Langmuir and Freundlich Isotherm models were used to evaluate the experimental data. Advanced analytical methods like Fourier Transform Infrared (FTIR), and Scanning Electron Microscopy (SEM) were used to characterize the synthesized resins[16,17].

Experimental Section

Materials and Chemicals

Tamarind kernel powder (TKP), *Citrullus Colocynthis* seed powder (CCSP), dioxane, cyanuric chloride, sodium bicarbonate, Aspartic acid, concentrated solution of NaOH.

Preparation of Tamarind Triazine Amino Butanedioic Acid (TTABA) Resin

Tamarind kernel powder was used as starting material. 0.1 mole of TKP was transferred to a round bottom flask containing 100 mL dioxane. Temperature was maintained as about 5°C by external cooling and stirred. Further 7.2 g cyanuric chloride was added to this solution. Then by adding sodium bicarbonate, pH was kept to 7-8. The whole mass was then stirred for 2 h. 0.1 mol of the Aspartic acid (amino acid) was added to above process and pH was brought to 8-9 by adding concentrated solution of NaOH. The temperature of the mixture was raised to 35 to 40°C and stirred vigorously by magnetic stirrer for 5 h. The derivative of tamarind named as tamarind triazine amino butanedioic acid (TTABA) resin thus formed was filtered and washed with distilled water. It was finally dried at 100°C for 6-8 h.

Preparation of Citrullus Triazine Amino Butanedioic Acid (CTABA) Resin

Citrullus colocynthis seed powder (CCSP) was used as starting material. 0.1 mol of CCSP was

transferred to a round bottom flask containing 100 mL dioxane. Temperature was maintained as about 5°C by external cooling and stirred. Further 7.2 g cyanuric chloride was added to this solution. Then by adding sodium bicarbonate, pH was kept to 7-8. The whole mass was then stirred for two hours.

0.1 mol of the Aspartic acid (amino acid) was added to above process and pH was brought 8-9 by adding concentrated solution of NaOH. The temperature of the mixture was raised to 35 to 40°C and stirred vigorously by magnetic stirrer for 5 h. The derivative of Citrullus named as Citrullustriazine amino butanedioic acid (CTABA) resin thus formed was filtered and washed with distilled water. It was finally dried at 100°C for 6-8 h.

Preparation of As(III) Solution

Standard 1000 ppb Arsenic Solution (1 µg /mL arsenic): 0.132 g of National Bureau of Standards arsenious oxide (As_2O_3) (pre-dried in a vacuum oven at 105 °C for 1 hour) was dissolvedin 10 mL of 10% sodium hydroxide solution. Then it was neutralized with 1N sulphuric acid solution, and added 20 mL in excess; diluted to 1-L volume with distilled water and mixed. 10 mL of the standard solution was pipetted in a 1-L volumetric flask, 20 mL of 1N sulphuric acid was added and further diluted to volume with distilled water[18].

Batch Adsorption Studies

Batch adsorption experiments were carried out as a function of metalloid As(III) concentration (50, 100, 150, 200, 250, and 300) µg /mL, pH (1 to 10), adsorbent dose (2 to 20) g, contact time (20, 40, 60, 80, 100, 120,140, 160, and 180) min, and particle size (150 µm). As shown in Table 1, only one affective parameter was changed at a time, while all other parameters kept constant. Metalloid-bearing solutions were permitted to settle after each run of tests, and the leftover metalloid ion solutions were filtered using Whatman no. 42 filter paper. Each sample was kept in 20 mL for leftover As(III) analysis.

After the experiment was completed, the concentration of the remaining ion As(III) was directly determined by atomic absorption spectroscopy.

Eq. (1) is utilized to determine the percentage of metalloid adsorption (in %) by adsorbents.

$$\%\ Removal\ of\ As\ (III) = \left(\frac{C_o - C_e}{C_o}\right) \times 100 \quad \ldots (1)$$

Where C_o and C_e are initial metalloid ion and equilibrium concentrations, respectively.

Chelation Isotherm

According to Langmuir's theory, the equations of nonlinear adsorption isotherm models can be represented as:

$$q_e = \frac{q_{max}\, b C_e}{1 + b C_e} \quad \ldots (2)$$

Eq.(2) can be rearranged by following linear form:

$$\frac{C_e}{q_e} = \frac{1}{b q_{max}} + \frac{1}{q_{max} C_e} \quad \ldots (3)$$

Where C_e is the equilibrium concentration, q_e is the amount of metalloid ion adsorbed, q_{max} is q_e for a complete monolayer (mgL^{-1}) and b is the sorption equilibrium constant (Lmg^{-1}). A graph of C_e versus C_e/q_e should indicate a straight line of slope $1/ q_{max}$ and an intercept of $1/ bq_{max}$ showing saturated monolayer adsorption.

Freundlich has found that if the concentration of solute in a solvent at equilibrium C_e (mgL^{-1}) was raised to the power of m, the amount of solute adsorbed being q_e, then C_e/q_e was found to be constant at a given temperature.

This satisfactory empirical isotherm can be used for non-ideal sorption and is expressed by the following equation in the form of a logarithm of both sides.

$$log q_e = log\ K_f + m\ log\ C_e \quad \ldots (4)$$

An adsorption isotherm is characterized by a certain constant, the value of which expresses the surface properties and affinity of the sorbent and can also be used to compare the bio-chemosorptive capacity of biomass for different metalloid ions[19].

Chelation Kinetics

Chelation kinetics is the study of the rate at which the solute particles get absorbed onto a solid surface, which is a critical component of adsorption

Table 1 — Experimental conditions

Experimental conditions	Ms (gL^{-1})	pH	Ps (µm)	T (min)	C_o (mgL^{-1})
Effect of adsorbent dosage Ms (gL^{-1})	2-20	4	150	120	50
Effect of pH	10	2-10	150	120	50
Effect of contact time T (min)	10	4	150	20-180	50
Effect of concentration of As (III)ion C_o (mgL^{-1})	10	4	150	120	50-300

processes. The models used to describe the kinetics of adsorption of As(III) on TTABA and CTABA resins include pseudo-first-order (PFO), pseudo-second-order (PSO), Intra-particle diffusion (IPD).[12,16]

The linearized equations of various kinetic models are represented here with their respective units:

PFO kinetics:

$$\ln(q_e - q_t) = \ln q_e - k_1 t \quad \ldots (5)$$

where, q_e is the amount of adsorbate adsorbed at equilibrium in mg g^{-1}, q_t is the amount adsorbed at time t in mg g^{-1}, k_1 is the rate constant of the PFO kinetics adsorption process in min^{-1} and, t is time in min.

PSO kinetics:

$$\frac{t}{q_t} = \frac{1}{k_2 q_e^2} + \frac{t}{q_e} \quad \ldots (6)$$

where, k_2 is the rate constant of the PSO kinetics adsorption process in g $mg^{-1}min^{-1}$.

Results and Discussion

Characterization of resins

FTIR Analysis

The chemical structure and functional groups of polysaccharide-based ion exchange resins of TTABA and CTABA were characterized with fourier transform infrared spectrometer[5]. The FTIR spectra (Fig. 1) showed different characteristic peaks of various functional groups present in resins of TTABA and CTABA, respectively. The strong broad band at 3447.03 cm^{-1} of TTABA resin and at 3269.45 $cm^{-1}$of CTABA resin represented the –OH stretching of hydroxyl group, the peak at 2924.55 cm^{-1} and at 2925.75 cm^{-1} corresponded to C-H stretching of the alkane of TTABA and CTABA resins, respectively. The presence of N-H component is attributed to the peaks found at 2355 cm^{-1} of TTABA resin and at 2467 cm^{-1}, 2370 cm^{-1} of CTABA resins, which show incorporation of amino acid during resin synthesis. The peak at 1747.73 cm^{-1} of TTABA resin and at 1715.86 cm^{-1} of CTABA resin were attributed to C=O stretching due to either acetyl or carboxylic group. The peak at 1270 cm^{-1} and at 1240 cm^{-1} represented the C-O-C asymmetric stretching of aryl-alkyl ether in the TTABA and CTABA resins, respectively. The peak at 1069 cm^{-1} and at 1062 cm^{-1} exhibited the C–O stretching of ethers functional group in TTABA and CTABA resins, respectively, Furthermore, the peak at 1402 cm^{-1} of TTABA resin and at 1405 cm^{-1} of CTABA resin showed symmetric stretching of COO-, C-N, at 1152 $cm^{-1}$of TTABA resin and at 1155.5 $cm^{-1}$of CTABA resin showed C-O, C-C stretching of C-O-C, ring. The presence of these functional groups shows that resins have ability to bind itself with heavy metal.

SEM

SEM (scanning electron microscopy) is a versatile and a powerful tool for characterisation of solid material, it produces detailed & magnified (2500x to 5000x) images of compounds which can be used to obtain information about surface's topography and

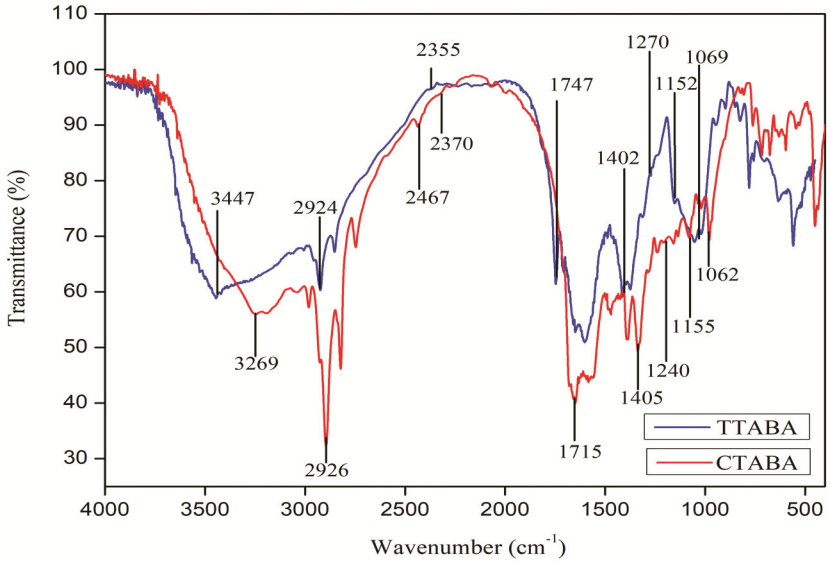

Fig. 1 — FTIR Spectra of TTABA and CTABA resins

composition[5]. SEM micrographs of resin TTABA and resin CTABA are shown in Fig 2 (a), (b) & (c), (d), respectively. The variation in the exterior morphology can be observed in the micrographs. Resin TTABA has tube shaped elongated particles whereas Resin CTABA has the spherical shaped particles with high porosity in both. As a highly un-organised porous structures are observed in electron micrograph of both the resins. The images reveal three-dimensional network structure with ample porosity, and these abundant and irregular pores are thought to be the regions of heavy metal ions trapping or active sites for interaction of heavy metal ions with chelating resins. There are multiple active sites of functional groups, which could chelate with metal ions immensely[20].

Effect of different parameters for As (III) removal

Effect of pH

Removal of As(III) ion from both TTABA resin and CTABA resin was performed separately with a pH change from 2 to 10 and other parameters were taken as constant like chelating resin dosage 10 gL^{-1}, As (III) concentration 50 mg L^{-1}, and time 120 min[21]. Removal of Arsenite ion was maximum at pH 4 for both resins. It was found 82.3% for TTABA and 75.6% for CTABA resin. Hydrogen ions become less abundant when pH rises. Thus, the interaction between metalloid and hydrogen ions also gets reduced and the removal of metalloid ions decreases as shown in Fig. 3 (a).

Effect of Concentration of As(III) Ion

The concentration of the As(III) metalloid ion was varied from 50 to 300 mg/L for adsorption investigation[22]. While other variables, such as the amount of chelating resin used (10 gL^{-1}), contact period (120 min) and pH 4 were kept constant. Fig. 3 (b) shows how the adsorption percentage drops as the quantity of metalloid ions is increased. Such behaviour may be caused by the unchanging number of available active sites on the chelating resin, here the amount of chelating resin is constant. Therefore, As(III) ions are left unbound in the solution due to the saturation of binding sites on the available chelating resin. For TTABA resin, As (III) ion removal efficiency falls from 82.3 to 76.1% and for CTABA resin it falls from 75.6 to 68.8%. It may be because there is not enough surface area to hold the original large number of ions. This shows that the sorption sites and ions interact more frequently at lower concentrations for increase in the removal efficiency.

Effect of Chelating Resin Dosage

Fig. 3 (c) illustrates the effect of chelating resin dosage on the removal of As(III), with dose ranging

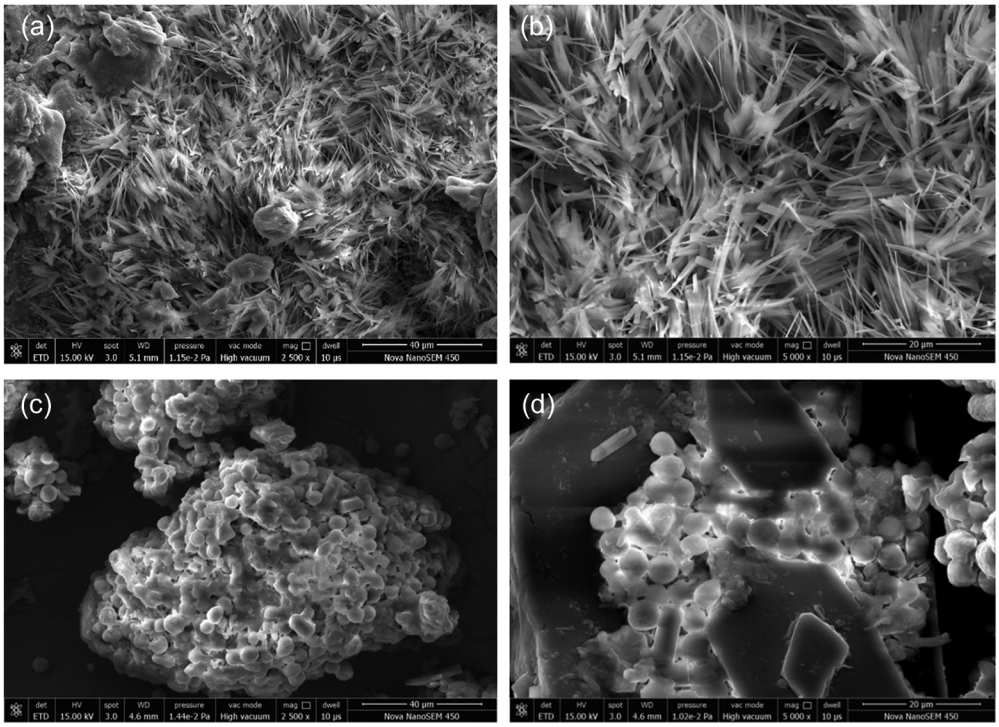

Fig. 2 —SEM micrographs of TTABA (a, b) and CTABA (c, d) resins

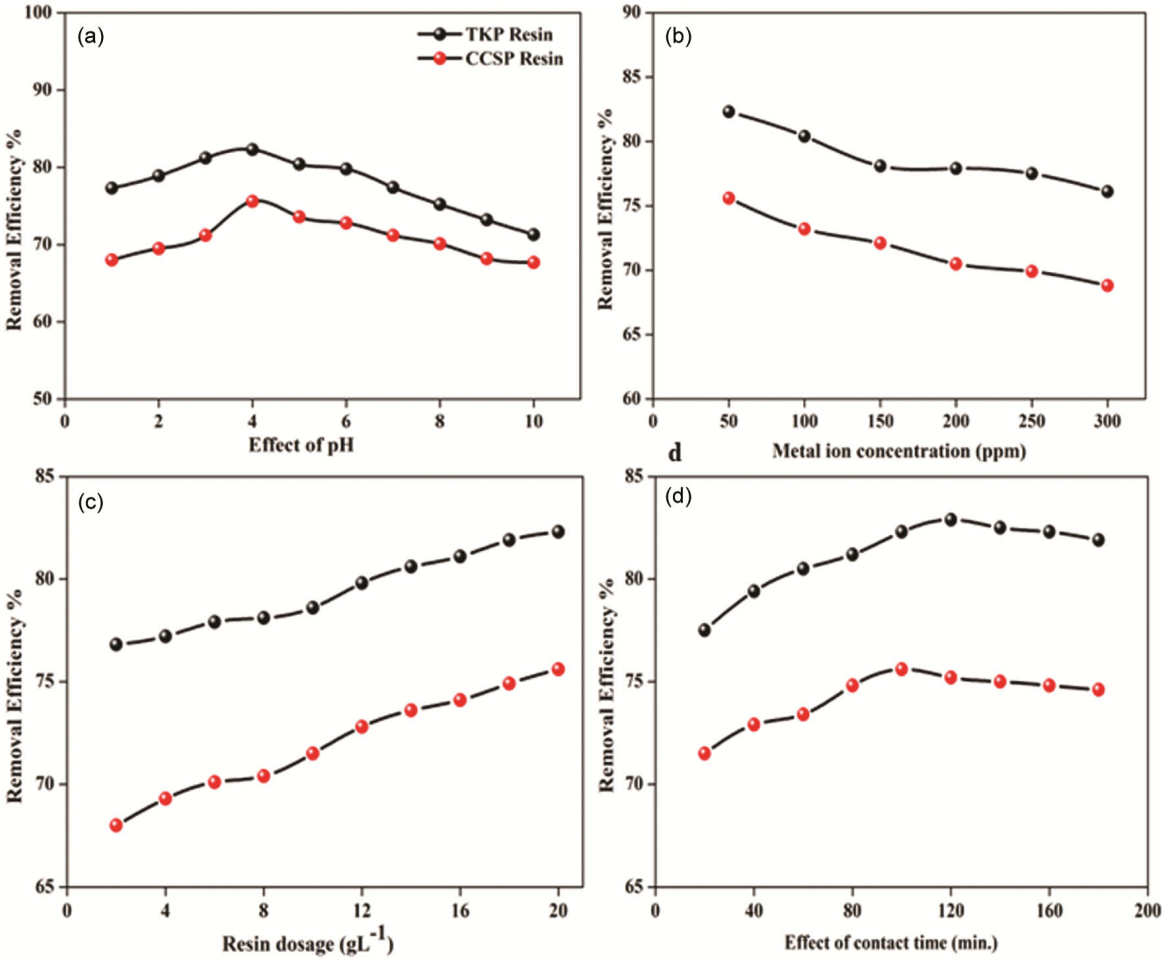

Fig. 3 —Effects of (a) pH, (b) metalloid ion concentration, (c) chelating resin dosage and (d) contact time on removal of As(III) ions

from 2 to 20 g L^{-1} while keeping other factors constant such as pH, contact period, and metalloid ion concentration[23]. The processes were applied using TTABA resin and CTABA resin with biomass dosages ranging from 2 to 20 g L^{-1}. The identical conditions were applied to both ion exchange resins. The removal efficiency improves along with the chelating resin's biomass. Increase in chelation with chelating resin dose can be associated with increase in chelating resin's surface area and availability of more ion interaction sites. The highest removal efficiencies of TTABA resin and CTABA resin have been found to be 82.3% and 75.6%, respectively.

Effect of Contact Time

Experiments were carried out with the change in the contact time (20-180) min while other parameters were kept constant i.e., pH 4, concentration of As(III) 50 mg L^{-1}, adsorbent dosage 10 g L^{-1} and particle size of biomasses 150 µm[25]. The results as shown in Fig. 3 (d) demonstrate that removal efficiency increases with the increase in contact duration because more time is available for metalloid ions to interact with chelating resin. However, because the effective period has already passed after 120 min, so further, the contact time does not demonstrate its effectiveness.

Isotherm Models of Chelation

The distribution of As(III) ions between two contacting phases is described mathematically by isotherm models. The distribution of both biosorbents (TTABA resin and CTABA resin) between the liquid and solid phases depends on how much the As(III) metalloid ion attracts them. The Langmuir and Freundlich isotherms were used to explain the experimental data as shown in Fig. 4[24,25].

The isotherm model parameters were estimated from the fitting of experimental point of As(III) adsorption as

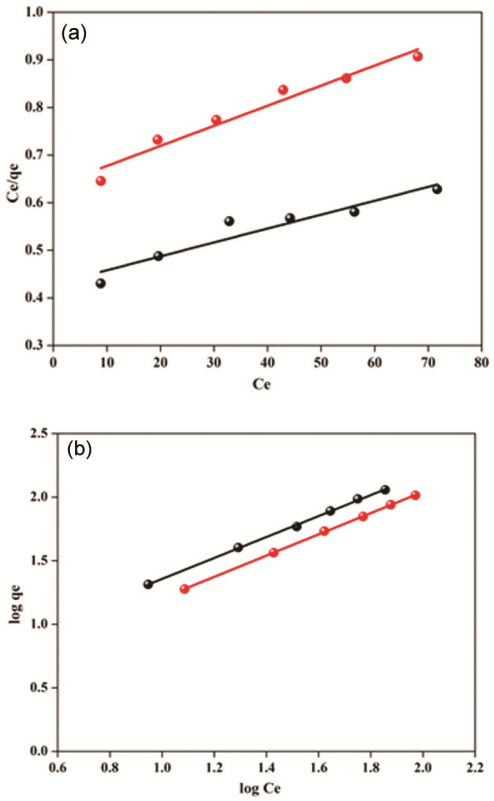

Fig. 4 — (a) Langmuir and Freundlich adsorption isotherm for TTABA (black colour) and CTABA (red colour) resin

Table 2 — Langmuir and Freundlich isotherms model parameters

Adsorbents	Langmuir isotherm			Freundlich isotherm		
	R^2	q_{max} (mg g^{-1})	b (L mg^{-1})	R^2	K_f (mg g^{-1})	m
CTABA Resin	0.961	322.58	0.0049	0.999	2.35	0.8357
TTABA Resin	0.911	344.82	0.0068	0.998	3.41	0.8240

reported in Table 2. As the regression coefficient values (R^2) are closer to one for both chelation models so not only monolayer adsorption due to chelation takes place but also multilayer adsorption is quite prominent for both resins due to presence of various functional group on polysaccharide chain of resin.

Adsorption kinetics of the Chelation

The study of adsorption kinetics focuses on the rate at which solute molecules attach to the surfaces of solid adsorbents. In investigating the kinetics of As(III) adsorption on TTABA and CTABA, various time-dependent kinetic models were employed, particularly the Pseudo-First-Order (PFO) and Pseudo-Second-Order (PSO) models. The PFO model suggests that physisorption is the main mechanism influencing the rate, while the PSO model considers the contribution of chemisorption.[12,26]

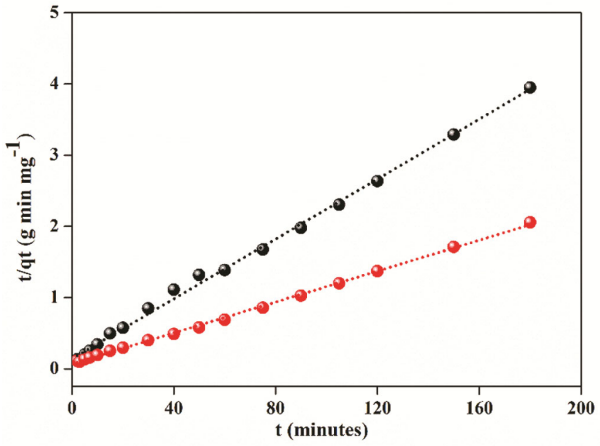

Fig. 5 — PSO kinetics plot for adsorption of As(III) on to TTABA (black colour) and CTABA (red colour) resin

Table 3 — Kinetic parameters obtained PSO model

Adsorbents	PSO			
	K_2	q_{exp}	q_{cal}	R^2
CTABA Resin	0.0012	13.21	15.79	0.9969
TTABA Resin	0.004	15.25	18.34	0.9971

Table 3 presents the kinetic parameters obtained from the two models being analysed. To assess the findings, it is crucial to compare the experimental data with the models' predictions. Notably, the PSO model shows higher correlation coefficient (R^2) values that approach one, especially at an initial As(III) concentration (C_0) of 50 mg L^{-1}. Additionally, the q_e values derived from the PSO model correspond closely with both the experimental and calculated values for TTABA and CTABA. This strong correlation indicates that the PSO model is the most dependable framework for understanding As(III) adsorption, emphasizing chemisorption as a significant mechanism on the surfaces of WR and NWR. The linear relationship of the PSO model with the experimental data is further illustrated in Fig. 5, which highlights the impressive R^2 values.

Conclusion

The present study demonstrates applications of TTABA resin and CTABA resin in removal of As(III) ion. This approach has been found to be simple process for effluent treatment using above polysaccharide-based ion exchangers resins. The maximum percentage removal of As(III) ion by both resins were observed at pH 4. The other conditions of maximum removal efficiencies were reported as contact time 120 min., chelating resin dose 10 g/L and at metalloid As(III) ion concentration 50 ppm for both resins. *Tamarind* kernel

based TTABA resin has been found as more efficient chelating resin for the removal of As(III) from wastewater as compared to *Citrullus colocynthis* seeds powder based CTABA resin. The maximum removal was found 82.3% for TTABA resin and 75.6% for CTABA resin. The experimental results have been analysed by Langmuir and Freundlich isotherms models. The adsorption data were found to be well fitted for both chelation isotherms, thus indicating the applicability of monolayer coverage as well as multilayer coverage of the As(III) ions on the surface of the chelating resin. Monolayer adsorption occurs due to formation of chemical bonds between chelating resin and As(III) while the interaction between As(III) and various functional groups on polysaccharide chain of resin is responsible for multilayer adsorption. The interaction of metal ions and carboxylate would change from covalent to ionic bond with increased number of chelating groups contained in resin as indicated by IR spectrum.

Acknowledgment

The authors are grateful to University Grant Commission, New Delhi, India for the award of Junior Research Fellowship.

References

1 Swami D & Buddhi D, Removal of contaminants from industrial wastewater through various non-conventional technologies: A review, *Int J Environ Pollut*, 27 (2006) 324.
2 Shrestha R, Ban S, Devkota S, Sharma S, Joshi R, Tiwari A P, Kim H Y & Joshi M K, Technological trends in heavy metals removal from industrial wastewater: A review, *J Environ Chem Eng*, 9 (2021) 105688.
3 Rashid R, Shafiq I, Akhter P, Iqbal M J & Hussain M, A state-of-the-art review on wastewater treatment techniques: The effectiveness of adsorption method, *Environ Sci Pollut Res*, 28 (2021) 9050.
4 Tchounwou P B, Yedjou C G, Patlolla A K & Sutton D J, Heavy metal toxicity and the environment, *Exp Suppl*, 101 (2012) 133.
5 Oliveira R C, Hammer P, Guibal E, Taulemesse J M & Garcia O, Characterization of metal-biomass interactions in the lanthanum(III) biosorption on Sargassum sp. using SEM/EDX, FTIR, and XPS: preliminary studies, *Chem Eng J*, 239 (2014) 381.
6 Komorowicz I & Barałkiewicz D, Determination of total arsenic and arsenic species in drinking water, surface water, wastewater, and snow from Wielkopolska, Kujawy-Pomerania, and Lower Silesia provinces, Poland, *Environ Monit Assess*, 188 (2016) 504.
7 Mohammed A K S, Jayasinghe S S, Chandana E P S, Jayasumana C & De-Silva P M C S, Arsenic and human health effects: A review, *Environ Toxicol Pharmacol*, 40 (2015) 828.
8 Mitra A, Chatterjee S & Gupta D K, Environmental arsenic exposure and human health risk, *Arsenic Water Resour Contam*, (2020) 103.
9 Nguyet P, Luu T L, Le N A, Ngan N T K & Trang N T H, Groundwater arsenic pollution in Vietnam: Current opinion on the mobilization and remediation, *Curr Opin Environ Sci Heal*, (2025) 100596.
10 Gupta V K, Ali I, Saleh T A, Nayak A & Agarwal S, Chemical treatment technologies for waste-water recycling-An overview, *RSC Adv*, 2 (2012) 6380.
11 Ahamad Z & Nasar A, Utilization of azadirachta indica sawdust as a potential adsorbent for the removal of crystal violet dye, *Sustain Chem*, 4 (2023) 110.
12 Solanki A, Ahamad Z & Gupta V, Upcycling waste biomass: Alkali-modified watermelon rind as a lignocellulosic bioadsorbent for copper ion removal, *Ind Crops Prod*, 224 (2025) 120340.
13 El-taweel R M, Mohamed N, Alrefaey K A, Husien S, Abdel-Aziz A B, Salim A I, Mostafa N G, Said L A, Fahim I S & Radwan A G, A review of coagulation explaining its definition, mechanism, coagulant types, and optimization models; RSM and ANN, *Curr Res Green Sustain Chem*, 6 (2023) 100358.
14 Al-Enezi G, Hamoda M F & Fawzi N, Ion exchange extraction of heavy metals from wastewater sludges, *J Environ Sci Heal Part A*, 39 (2004) 455.
15 Chen C, Chiang C & Chen C, Removal of heavy metal ions by a chelating resin containing glycine as chelating groups, *Sep Purif Technol*, 54 (2007) 396.
16 Meena H M, Kukreti S & Jassal P S, Adsorption and estimation of As (III) from wastewater using cross linked Chitosan-STPP nanoparticles with voltammetric analysis computrace, isotherms, and kinetic study, *Results Eng*, 23 (2024) 102467.
17 Meena H M, Kukreti S & Jassal P S, Synthesis of a novel chitosan-TiO_2 nanocomposite as an efficient adsorbent for the removal of methylene blue cationic dye from wastewater, *J Mol Struct*, 1319 (2025) 139420.
18 Leblebici J & Volkan M, Sample preparation for arsenic, copper, iron, and lead determination in sugar, *J Agric Food Chem*, 46 (1998) 173.
19 Ali R M, Hamad H A, Hussein M M & Malash G F, Potential of using green adsorbent of heavy metal removal from aqueous solutions: Adsorption kinetics, isotherm, thermodynamic, mechanism and economic analysis, *Ecol Eng*, 91 (2016) 317.
20 Bargujar S, Gambhir G, Raigar M B, Hooda S, Arya D K & Bhatia M, A new polysaccharide-based ion-exchange resin for industrial wastewater treatment, *Polimery*, 67 (2022) 212.
21 Schiewer S & Patil S B, Modeling the effect of pH on biosorption of heavy metals by citrus peels, *J Hazard Mater*, 157 (2008) 8.
22 Wang Y H, Lin S H & Juang R S, Removal of heavy metal ions from aqueous solutions using various low-cost adsorbents, *J Hazard Mater*, 102 (2003) 291.
23 Jiang J, Ma X S, Xu L Y, Wang L H, Liu G Y, Xu Q F, Lu J M & Zhang Y, Applications of chelating resin for heavy metal removal from wastewater, *e-Polymers*, 15 (2015) 161.
24 Bulut Y & Tez Z, Removal of heavy metals from aqueous solution by sawdust adsorption, *J Environ Sci*, 19 (2007) 160.
25 Kapoor A, Viraraghavan T & Cullimore D R, Removal of heavy metals using the fungus Aspergillus niger, *Bioresour Technol*, 70 (1999) 95.
26 Ahamad Z, Ahmed M, Mashkoor F & Nasar A, Chemically modified Azadirachta indica sawdust for adsorption of methylene blue from aqueous solutions, *Biomass Convers Biorefin*, 14 (2023) 19929.